Materials Science Forum *Online: 2009-12-03*
ISSN: 1662-9752, Vol. 635, pp 155-160
doi:10.4028/www.scientific.net/MSF.635.155

Structural and magnetic properties of epitaxial Ni_2MnGa thin films

Tobias Eichhorn[1, a], Gerhard Jakob[1,b]

[1]Institute for Physics, Johannes Gutenberg University, 55099 Mainz, Germany

[a]tobiasei@students.uni-mainz.de, [b]jakob@uni-mainz.de

Keywords: Ni_2MnGa, epitaxial thin films, free-standing, martensitic transformation, 7M structure

Abstract

We report on the preparation and investigation of epitaxial thin films of the magnetic shape memory alloy Ni_2MnGa. For samples close to the stoichiometric composition we find that the phase transformation temperature is affected by the crystallographic orientation. Changes in the crystal structure due to the transformation are observed using temperature-dependent X-ray diffraction. Films with higher manganese content are in the martensitic state at room temperature. Those samples on Al_2O_3(11-20) reveal the 7-layered orthorhombic structure that allows strains up to 10 %. To avoid blocking of magnetostrictive effects by the substrate, free-standing films are prepared using water-soluble NaCl(100) single crystals as substrate.

Introduction

Since the discovery of the magnetic shape memory (MSM) effect in Ni_2MnGa single crystals [1] this compound has attracted increasing scientific interest. Among the alloys crystallizing in the $L2_1$ Heusler structure the Ni-Mn-Ga system has the particular feature of undergoing a martensitic phase transition. In the process the crystal structure changes from the cubic austenite to the tetragonal or orthorhombic martensite, where different crystallographic variants are separated by twin boundaries. These twin boundaries are highly mobile and can be moved through the crystal by the driving force of an external magnetic field. Such a magnetically induced reorientation (MIR) of variants is possible due to the coupling of the magneto crystalline anisotropy axes to the axes of the tetragonal or orthorhombic distortion. If the energy for twin boundary motion is less than that for magnetic rotation, MIR of variants can be observed. Adjacent variants with different orientation will increase or decrease in the volume fraction depending on the direction of the external field **H** resulting in minimization of Zeeman energy (**M**·**H**). Macroscopically the reorientation of variants leads to huge strains that can amount to 10 % in Ni_2MnGa single crystals [2]. According to that MSM alloys are promising materials for technical applications as actuators or sensors. On the basis of epitaxial thin films also micro devices could be realized. Since rigid substrates will block magnetically induced strains of the MSM alloy, free-standing films are needed. A simple alternative to sophisticated etching techniques as reported in [3] is deposition on soluble substrates as suggested by Hakola et. al. [4]. Another approach is deposition on thin metal foils or polyvinyl alcohol substrates as reported by Chernenko et. al. [5] or partly release the film by cutting out a cantilever with a focused ion beam [6].

Experimental details

The investigated samples are prepared by DC magnetron sputter deposition. As substrate materials Al_2O_3(11-20), MgO(100) and NaCl(100) single crystals are used. The substrate is heated to 500-600 °C for metal oxides and to 480 °C for sodium chloride respectively. The Ar sputter pressure is kept at 0.01 mbar, while the base pressure of the chamber is in the range of 10^{-8} mbar. Additionally a cold trap and a titanium cathode sputtering onto the liquid nitrogen cooled surface prevent oxidation of the Heusler compound during deposition. The homemade sputtering cathodes are equipped with two different alloy targets, one stoichiometric Ni_2MnGa, the other of the nominal

composition $Ni_{1.96}Mn_{1.22}Ga_{0.82}$. Typical parameters are 100 mA current at 330 V voltage for a argon pressure of 0.01 mbar. The distance between target and substrate is approximately 30 mm resulting in a deposition rate of 1.3 nm/s. The films on rigid substrates have a typical thickness of 100 nm, while samples prepared on NaCl are 0.5 to 1.5 µm thick. Those films can be detached from the substrate by dissolving it in distilled water.
Information on the crystal structure of the samples is gained by X-ray diffraction (XRD) using a commercial Phillips X'PERT instrument in Bragg-Brentano geometry and a homemade four circle rotating anode system. While XRD in 2-circle geometry only scans the out-of-plane orientation the four circle set up facilitates mapping of the whole reciprocal space. Furthermore the latter can be equipped with He-gas cryostat that allows cooling of the sample down to 20 K. The high temperature XRD measurements were performed in a Siemens D 5000 diffractometer.
The magnetic properties of the films are investigated with a superconducting quantum interference device (Quantum Design) and an Oxford instruments vibrating sample magnetometer.

Results and discussion

Samples prepared on Al_2O_3(11-20) using the stoichiometric target show a single (220) peak in the Bragg-Brentano scan confirming epitaxial growth of the cubic austenite phase of the Heusler compound. The in-plane alignment as indicated by the reciprocal space map of a plane perpendicular to the specular (220) reflection is $Ni_2MnGa[100]||Al_2O_3[1\text{-}100]$ as reported in [7].
MgO(100) substrates on the contrary induce (100) out-of-plane growth with a $Ni_2MnGa[110]||MgO[100]$ in-plane orientation (s. Fig 1) as also reported by Thomas et. al. [8]

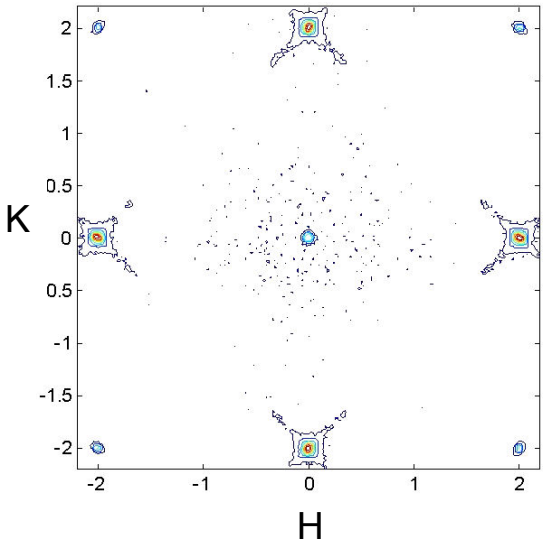

Fig. 1: Contour plot of *h k* scans with *l*=4 measured on Ni_2MnGa film on MgO(100).The fourfold symmetry of the cubic austenite is visible.

The films are $L2_1$ ordered and show no impurity phases. Rocking curve widths of the (220) reflection on sapphire and the (400) peak on MgO respectively are below 0.5° affirming the single crystalline character of the films.
The phase transformation of the films can be observed by temperature dependent XRD. When entering the martensitic phase the intensity of the (400) reflection is reduced due to the distortion of the cubic Ni_2MnGa lattice (s. Fig 2).

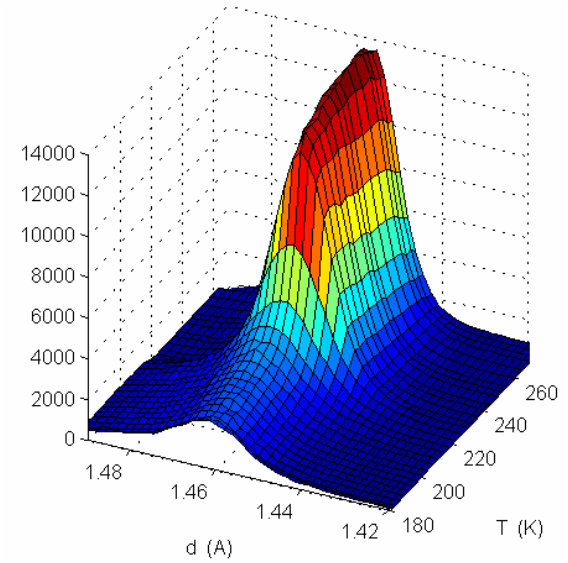

Fig 2: 3D plot of (*h*00) scans of the (400) XRD peak of a Ni_2MnGa film on MgO(100) substrate. Each scan is measured at constant temperature. The decrease in intensity indicates the onset of the martensitic transformation.

For the (100) oriented samples on MgO the transformation temperature (T_M) lies around 220 K while the corresponding films on sapphire have a T_M of 275 K [9]. This dependence of T_M from the crystallographic orientation of the sample is also present in the magnetization of the shape memory alloy. Fig. 3 shows the in-plane magnetization in a field of 10 mT as a function of temperature for two samples that were prepared simultaneously in a homogeneous sputtering plasma.

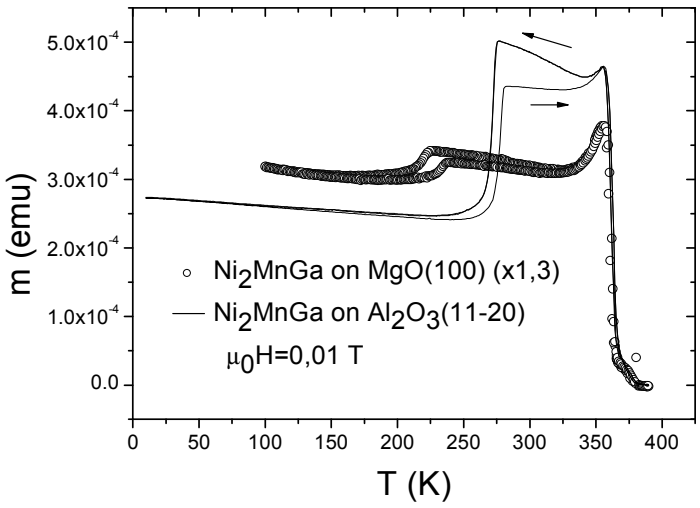

Fig. 3: In-plane magnetization vs. temperature in low field for two films with a different crystallographic orientation. The Curie temperature of the two samples corresponds while the drop indicating the phase transformation occurs at different temperatures.

The drop in the magnetization indicating a change in the in-plane anisotropy at the phase transition occurs at different temperatures for the sample on MgO(100) and Al_2O_3(11-20) coinciding the values obtained by XRD. Since compositional effects can be excluded this discrepancy in T_M is clearly attributed to the different crystallographic orientation. For films on MgO(100) all possible twin planes between the martensitic variants will hit the substrate surface

either under 45° or 90°. However on Al_2O_3(11-20) substrates the twin planes can run also parallel to the surface resulting in less interference between the twin boundaries and the substrate. This is reflected in the higher transition temperature of approximately 275 K for the (110) oriented samples while the Curie temperature is 370 K independent from the chosen substrate. In addition effects of epitaxial strain cannot be excluded as the film on MgO shown in Fig. 2 has a tetragonal strain of 1% at room temperature, whereas other samples with similar transition temperatures show no tetragonal strain.

Films prepared from the $Ni_{1.96}Mn_{1.22}Ga_{0.82}$ target are in the martensitic state at room temperature, which is not evident from XRD patterns measured with the two circle diffractometer. The position of the (400) Heusler peak on MgO(100) is hardly affected by the different stoichiometry. For films on Al_2O_3(11-20) a slight shift in the position of the (220) Ni_2MnGa reflection from 44.0° (for films sputtered from the stoichiometric target) to 44.3° in 2θ is observed. To investigate the structural changes during the transformation to the cubic parent phase a film on sapphire was heated from room temperature to 400 °C performing 2θ–θ scans in steps of 20 K (s. Fig. 4). Above 120 °C the peak maximum shifts from 44.3 ° towards 44.0 ° (for a cubic system this would change a from 5.78 to 5.82Å) and the intensity increases significantly indicating the transition to the austenite. The decrease in intensity for temperatures higher than 300 °C is attributed to beginning oxidation of the alloy since there is no inert atmosphere.

The detailed crystal structure of the martensite is revealed by XRD in four circle geometry. To obtain sufficient count rates a film of 800 nm thickness was prepared on Al_2O_3(11-20). Besides the single (220) specular reflection two sets of (202), (20-2) and (022), (02-2) peaks are observed at room temperature. These peaks are shifted in respect to those of the cubic lattice and fit to two orthorhombic variants with measured lattice parameters a_1=6.120Å; b_1=5.443 Å; c_1=5.753 Å; α_1=89.90°; β_1=89.89°; γ_1=90.03° and a_2=5.440Å; b_2=6.135 Å; c_2=5.760 Å; α_2=89.99°; β_2=89.96°; γ_2=90.16°. The slight mismatch of the lattice parameters is due to limited resolution. The assignment of the axes has been chosen to keep the (110) scattering vectors of the martensite and austenite parallel and perpendicular to the substrate.

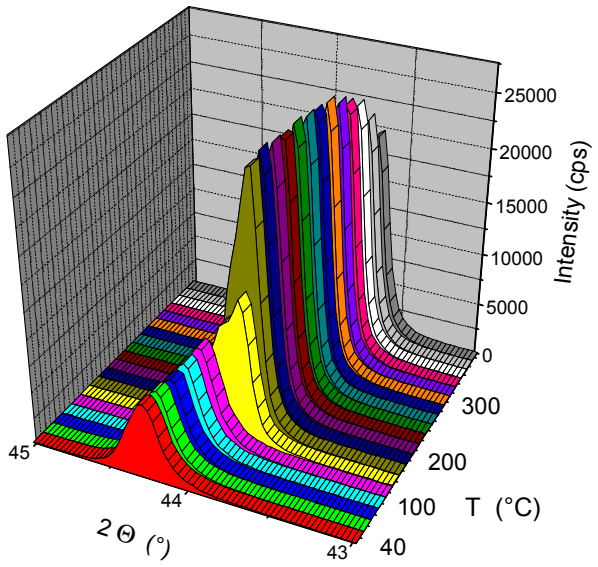

Fig. 4: Bragg-Brentano scans of a film prepared from a $Ni_{1.96}Mn_{1.22}Ga_{0.82}$ target on Al_2O_3(11-20) for different temperatures. The increase in intensity with increasing temperature indicates the transformation from martensite to austenite. Decrease of intensity above 300 °C is due to oxidation of the MSM alloy.

Along the [110] direction the length changes of a- and b-axes of a given variant with respect to the cubic phase compensate resulting in nearly the same position of the (220) reflection in austenite and martensite. This compensation can not occur for peaks with unequal *h* and *l*. Therefore peaks

with (*hhk*) indices are observed non-split, whereas (*hkl*) reflections are observed twofold originating from the two different variants of the martensite.

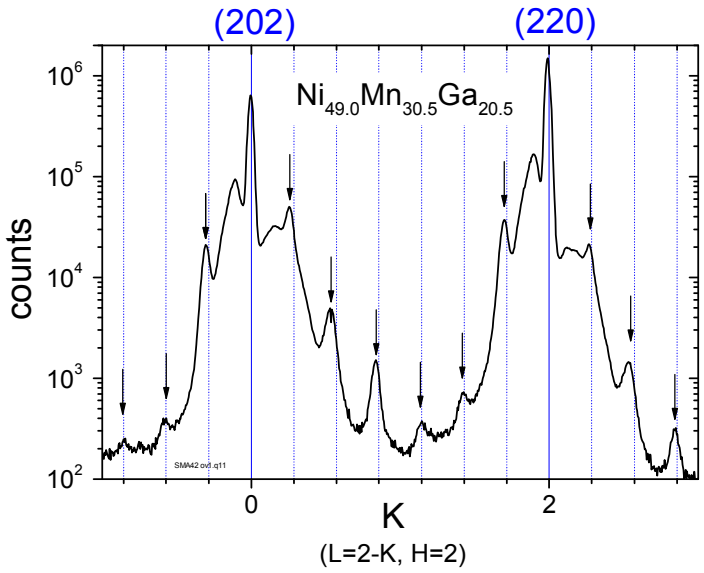

Fig. 5: XRD Line scan along a (01-1) direction in the reciprocal space performed on a film with the nominal (target) composition $Ni_{1.96}Mn_{1.22}Ga_{0.82}$ on Al_2O_3(11-20). Between the (202) and the (220) reflection six satellite peaks appear confirming the 7-layered orthorhombic structure for this sample.

The crystal structure of both variants is not simple orthorhombic but also shows modulation of lattice planes with a period of 14 layers, the so called 7M structure [10]. This is evident when scanning in the reciprocal space along a line from the (202) to the (220) reflection (s. Fig. 5). Along the [01-1] direction six equidistant satellite peaks appear coinciding with the 7M structure. The additional intensity measured close to the (202) and (220) reflection is caused by contribution of the second variant to the diffraction. The modulation is also present in [0-1-1] direction but is not observed for lattice planes normal to [10-1] and [-101].

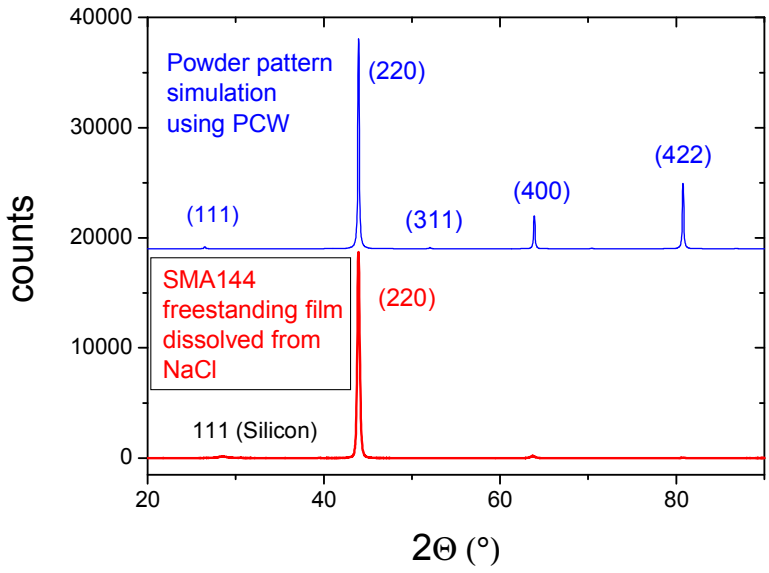

Fig. 6: Bragg-Brentano scan of a free-standing $Ni_{2.11}Mn_{1.23}Ga_{0.66}$ film detached from the NaCl(100) substrate (lower curve) in comparison to a powder pattern simulation. The film shows a strong (110) out-of-plane texture as evident from the strong (220) reflection.

Films prepared on NaCl(100) substrates grow in the cubic austenite phase. When cooling down to the martensite the induced stress leads to corrugation and partial detachment of the film. Due to the wavy surface XRD measurements are complicated even for released films. Fig. 6 shows a 2θ–θ scan of a free-standing $Ni_{2.11}Mn_{1.23}Ga_{0.66}$ film sitting on a silicon substrate in comparison to the powder pattern simulation using *Powder Cell 2.4* software. Besides the weak (400) reflection there is pronounced (110) out-of-plane orientation which is quite astonishing since the substrate is cut along [100]. The ω-scan of the (220) peak reveals a width of 4.5 ° indicating the strongly textured growth of the Heusler compound. Recently Heczko et al. reported on films with a composition of $Ni_{2.04}Mn_{0.92}Ga_{1.04}$ prepared on NaCl(100) at 300 °C that exhibit (100) orientation [11]. In our case energy dispersive X-ray analysis indicates a film composition of $Ni_{2.11}Mn_{1.23}Ga_{0.66}$.

Conclusions

Structural and magnetic properties of NiMnGa epitaxial thin films of two different compositions were investigated. Films close to stoichiometric composition show a phase transformation temperature that depends on the crystallographic orientation. The samples prepared from a target with manganese excess are in the martensitic phase at room temperature showing the 7-layered orthorhombic structure. Two symmetric variants have been observed revealing modulation along [01-1] and [0-1-1], but not along [10-1] and [-101] directions. For both types of thin films changes in the crystal structure due to the phase transition were detected by temperature-dependent X-ray diffraction. Furthermore we prepared free-standing films with a strong (110) texture using NaCl(100) substrates.

References

[1] K. Ullakko, C. Kantner, R. C. O'Handley and V. V. Kokorin, Appl. Phys. Lett. **69**, 1966 (1996)

[2] A. Sozinov, A. A. Likhachev, N. Lanska and K. Ullakko, Appl. Phys. Lett. **80**, 1746 (2002)

[3] J. W. Dong, L. C. Chen, C. J. Palmstrom, R. D. James and S. McKernan, Appl. Phys. Lett. **75**, 1443 (1999)

[4] A. Hakola, O. Heczko, A. Jaatinen, V. Kekkonen and T. Kajava, Journal of Physics: Conference Series **59**, 122–125 (2007)

[5] V. A. Chernenko, R. L. Anton, M. Kohl, J. M. Barandiaran, M. Ohtsuka, I. Orue, and S. Besseghini, Acta Mat. **54**, 20, 5461-5467 (2006)

[6] C. A. Jenkins, R. Ramesh, M. Huth, T. Eichhorn, P. Pörsch, H. J. Elmers and G. Jakob, Appl. Phys. Lett. **93**, 234101 (2008)

[7] G. Jakob, T. Eichhorn, M. Kallmayer and H. J. Elmers, Phys Rev B **76**, 174407 (2007)

[8] M. Thomas, O. Heczko, J. Buschbeck, U.K. Rößler, J. McCord, N. Scheerbaum, L. Schultz and S. Fähler, New J. Phys. **10**, 023040 (2008)

[9] G. Jakob and H. J. Elmers, Magn Magn Mat **310**, 2779 (2007)

[10] V. V. Martynov, V. V. Kokorin, J. Phys. III France **2**, 739-749 (1992)

[11] O. Heczko, M. Thomas, R. Niemann, L. Schultz and S. Fähler, Appl. Phys. Lett. **94**, 152513 (2009)